IL NUOVO CIMENTO **48 C** (2025) 49
DOI 10.1393/ncc/i2025-25049-6

Colloquia: IWM-EC 2024

Latest results of data analysis related to FARCOS correlator in the CHIFAR experiment

C. Zagami(1)(2)(3), E. V. Pagano(2), P. Russotto(2), E. De Filippo(4), L. Acosta(5)(6), T. Cap(7), G. Cardella(4), F. Fichera(4), E. Geraci(1)(4)(3), B. Gnoffo(1)(4), C. Guazzoni(9)(10), G. Lanzalone(11)(2), C. Maiolino(2), N. S. Martorana(4), T. Matulewicz(8), A. Pagano(4), M. Papa(4), K. Piasecki(8), S. Pirrone(4), M. Piscopo(2), R. Planeta(12), G. Politi(1)(4), F. Risitano(13)(4), F. Rizzo(1)(2)(3), G. Saccà(4), G. Santagati(4), K. Siwek-Wilczynska(8), I. Skwira-Chalot(8) and M. Trimarchi(13)(4)

(1) *Dipartimento di Fisica e Astronomia "Ettore Majorana", Università di Catania Catania, Italy*
(2) *INFN, Laboratori Nazionali del Sud - Catania, Italy*
(3) *CSFNSM-Centro Siciliano di Fisica Nucleare e Struttura della Materia - Catania, Italy*
(4) *INFN, Sezione di Catania - Catania, Italy*
(5) *Instituto de Física, Universidad Nacional Autónoma de México - Mexico City, Mexico*
(6) *Instituto de Estructura de la Materia, CSIC - Madrid, Spain*
(7) *National Centre for Nuclear Research - Otwock, Poland*
(8) *Faculty of Physics, University of Warsaw - Warsaw, Poland*
(9) *Dip. di Elettronica, Informazione e Bioingegneria, Politecnico di Milano - Milano, Italy*
(10) *INFN, Sezione di Milano - Milano, Italy*
(11) *Facoltà di Ingegneria e Architettura, Università Kore - Enna, Italy*
(12) *M. Smoluchowski Institute of Physics, Jagiellonian University - Krakow, Poland*
(13) *Dipartimento di Scienze MIFT, Università di Messina - Messina, Italy*

received 26 November 2024

Summary. — The CHIFAR experiment, carried out at Laboratori Nazionali del Sud-INFN, aims to study the reaction mechanisms and Intermediate Mass Fragments (IMFs) emission probability in non-central Heavy-Ion collisions. These phenomena are linked to the features of the Equation of State of the nuclear matter, and shine light also on the role of the isospin degree of freedom of the colliding nuclei. In the CHIFAR experiment, nuclear reactions at incident beam energy of 20 AMeV were investigated using different combinations of beams: ^{124}Sn, ^{112}Sn and ^{124}Xe, and targets: ^{64}Ni, ^{58}Ni and ^{64}Zn, in order to study combinations of neutron-rich and neutron-poor systems. The experimental setup was equipped with ten telescopes of the FARCOS correlator, coupled with the 4π CHIMERA multi-detector. This coupling allowed the study of the correlations between IMFs and light charged particles emitted in a nuclear reaction. The results on the energy calibration, on the energy resolution and on the identification of the detected particles by FARCOS correlator used in the CHIFAR experiment are explained. Some preliminary results regarding the physics cases studied in the experiment are also reported.

1. – Introduction

The CHIMERA Collaboration studied Heavy-Ion (HI) collisions at intermediate energy regime (10 $\text{MeV}/A < E/A < 100$ MeV/A), using mainly the CHIMERA detection system [1], operating at INFN-LNS, aimed at detecting simultaneously multiple charged reaction products. Thanks to the CHIMERA multi-detector high performances, the Collaboration studied deeply the semi-periferal collisions, detecting simultaneously the Projectile-Like Fragment (PLF), the Target-Like Fragment (TLF), the Intermediate Mass Fragments (IMFs), and also the associated Light Charged Particles (LCPs). The so-called "neutron-rich" nuclear system $^{124}\text{Sn} + {}^{64}\text{Ni}$ and the so-called "neutron-poor" one $^{112}\text{Sn} + {}^{58}\text{Ni}$ were studied at 35 AMeV beam energy in the previous REVERSE experiment [2]. In the following InkiIsSy experiment [3], other two nuclear reactions were investigated at the same incident beam energy: the $^{124}\text{Xe} + {}^{64}\text{Zn}$, which is an isobaric combination of the neutron-rich one with the isospin contribution similar to the neutron-poor one, and the $^{124}\text{Xe} + {}^{64}\text{Ni}$. Data analysis of these experiments highlighted some important results: the fast dynamical emission is favoured in the neutron-rich system; furthermore, the isospin content, characterized by the ratio N/Z, plays an important role in the reaction's dynamics. The IMFs emission probability grows with the isospin content of both, projectile and target, nuclei. The enhanced IMFs emission in the neutron-rich systems originates from an enhancement of the dynamical emission. Thus, the influence of the isospin content is relevant in triggering the dynamical emission mechanism, while it can be excluded that the mass difference gives a significant contribution in the dynamical IMFs emission.

The CHIFAR experiment [4] was carried out at INFN-LNS in 2019. The experiment investigated the emission probability of the IMFs in non-central collisions, in order to estimate the dynamical or statistical contributions of the emission processes, and their dependence on the isospin content of projectile and target. Six nuclear reactions, at 20 AMeV beam energy, were obtained from different combinations of beams —^{124}Sn, ^{112}Sn, ^{124}Xe— and targets —^{64}Ni, ^{58}Ni, ^{64}Zn— in order to study the combinations of neutron-rich and neutron-poor systems. Table I shows the isospin values for each studied collision.

2. – The CHIFAR experimental setup

The experimental setup used in the CHIFAR experiment was formed by the coupling between the Femtoscope ARray for COrrelation and Spectroscopy (FARCOS) correlator and the 4π multi-detector CHIMERA.

FARCOS [5,6] is a new generation correlator, characterized by high energy and angular resolution. It consists of 20 telescopes, and it has a modular array structure. Figure 1 shows the cluster of each telescope. The first two stages are composed by Double Sided Silicon Strip Detectors (DSSSDs), 300 μm and 1500 μm thick, respectively, that have 32 vertical strips in the front side and other 32 horizontal strips in the back one, with an active area of 6.4×6.4 cm^2; then, 4 CsI(Tl) crystals are used in the third stage of the telescope, having 6 cm thickness and an active area of 3.2×3.2 cm^2. During the CHIFAR experiment, the experimental setup included 10 telescopes of FARCOS correlator, covering the laboratory angles between 13° and 30°. The signals were processed by ASIC preamplifiers [7] and digitized with the GET electronics [8].

The CHIMERA multi-detector is made of 1192 telescopes, arranged into 35 total rings, with a forward part that covers the polar angle range 1°–30° with a cylindrical

Table I. – *Isospin values of nuclear reactions studied in the CHIFAR experiment.*

		$I_P = N_P/Z_P$	$I_T = N_T/Z_T$	$I_{\text{reaction}}^{\text{mean}} = N/Z$
"neutron-rich"	^{124}Sn + ^{64}Ni	1.48	1.29	1.38
"neutron-poor"	^{112}Sn + ^{58}Ni	1.24	1.07	1.16
"isobaric"	^{124}Xe + ^{64}Zn	1.30	1.13	1.21
	^{124}Sn + ^{64}Zn	1.48	1.13	1.31
	^{112}Sn + ^{64}Ni	1.24	1.29	1.26
	^{124}Xe + ^{64}Ni	1.30	1.29	1.29

geometry along the beam and a sphere covering 30° to 176° polar range. Each telescope is formed by a Si detector (300 μm thick) and a CsI(Tl) scintillator (3–12 cm of thickness). Two important features of CHIMERA are the high granularity and the large solid angle coverage. The typical energy resolution (FWHM), evaluated by elastic scattering, is around $\Delta E/E < 1\%$ for the Si detectors and about 2% for the CsI(Tl) scintillators [9]. Particles identification methods can be applied and the events can be reconstructed with very good accuracy [10]. CHIMERA allowed to study different phenomena related to the reaction dynamics, such as the neck fragmentation in ternary events (PLF + TLF + IMFs) [11], or the dynamical fission of the PLF [12], and with references to the nuclear structure and nuclear astrophysics such as Pygmy Dipole Resonance [13] or Hoyle state and higher energy levels in ^{12}C [14, 15].

According to the features described, CHIMERA is able to provide a complete characterization of the reaction events, and FARCOS gives a very precise identification of the detected fragments in its limited solid angle coverage thanks to its high resolution.

3. – Data analysis and selected preliminary results

3·1. *Energy calibration of the DSSSDs.* – The so-called "punching-through" technique was applied in the first step of the data analysis, in order to obtained the energy calibration of the first two stages (DSSSDs) of FARCOS telescopes. For each couple of DSSSDs, the $\Delta E - E$ matrix shows some tails at the end of the hyperbolic curves generated by the detected particles. It means that the particles are passing through the second DSSSD and they lose completely their remaining energy in the last CsI(Tl) detectors. The snap backs are more visible in correspondence of the ^{7}Li, ^{7}Be and ^{9}Be curves. This allows for clear identification of such fragments in the $\Delta E - E$ matrix (see fig. 2). The to-

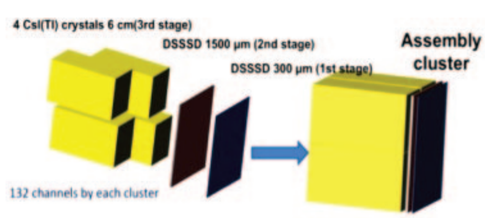

Fig. 1. – Schematic representation of a cluster of FARCOS [5].

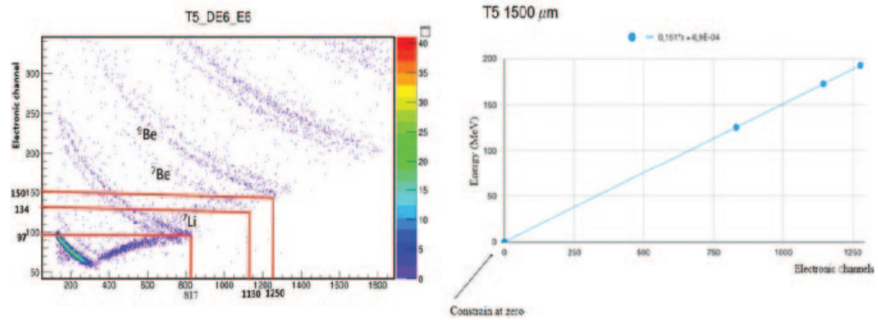

Fig. 2. – Punching-through points are indicated in the $\Delta E - E$ identification matrix of the front side of one of the Si detectors (left panel). Energy calibration of the module assuming linear dependence (right panel).

tal kinetic energy released by each fragment was evaluated using LISE++ program [16] assuming that the final energy was equal to zero at the end of the path in the two DSSSDs (1800 μm). From the linear best fit, the calibration parameters were determined for each FARCOS telescope. After that, the DSSSDs back side strips were calibrated by using the front side ones. Figure 2 shows the application of the "punching-through" method.

3˙2. *Energy resolution of the DSSSDs*. – The evaluation of the DSSSDs front side energy resolution was obtained by using elastically scattered ions from three reactions: ^{16}O + ^{197}Au at 85 MeV beam energy and ^{12}C + ^{197}Au at 75 and 65 MeV. All beams were provided by tandem accelerator. The average energy released in each telescope was estimated from the Gaussian fit to the elastic peaks. An energy resolution around 0.5% RMS (corresponding to 1.5 MeV at 300 MeV of peak) was achieved, better for the higher energy of the three considered ones. The linear proportionality between the FWHM and the square root of the energy released was verified for each telescope. The total error of energy measured in the DSSSDs was around 1.5 MeV. The intrinsic component of the energy resolution and the electronic one were calculated, in order to verify that approximately 80% of the total error was due to the electronic chain, *e.g.*, the preamplifier, the digitizer and also any error coming from the entire experimental setup. Concerning the DSSSDs back side energy resolution, the ratio $(\Delta E_{\mathrm{front}} - \Delta E_{\mathrm{back}})/\Delta E_{\mathrm{front}}$ was useful to estimate an energy resolution around 1.6% RMS (corresponding to 4.8 MeV at 300 MeV of peak), having considered each front strip in coincidence with all 32 back strips.

3˙3. *Particle identification phase*. – The $\Delta E - E$ technique was applied in the phase of data analysis concerning the identification of detected particles by the two DSSSDs of FARCOS telescopes. Some experimental constraints were imposed to select particles having multiplicity equal to one in both sides of the first DSSSD and also in the front side of the second DSSSD; particles have to stop in one of the two Si detectors, to have the multiplicity relative to the CsI(Tl) crystals equal to zero. The energy released in the front side of the first DSSSD should be approximately the same, within the energy resolution of the two sides, as the energy lost in the back side; therefore, the experimental range of the acceptance for the selected events was restricted to ±15%, in order to maintain a good statistic. The last imposed constraint was related to the stripes hit by the particles:

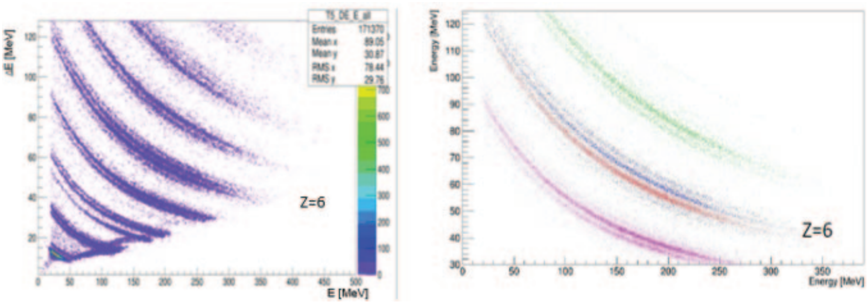

Fig. 3. – $\Delta E - E$ matrix identification for the telescope No. 5 (left panel); the zoom highlights the good separation in charge and mass, *e.g.*, for the IMFs with atomic number $Z = 6$ (right panel).

they must be the same, or at most adjacent, between the two DSSSDs front sides. After the selection of these conditions, an automatic algorithm, developed by the CHIMERA Collaboration and based on the Bethe-Bloch formula, was applied to the $\Delta E - E$ matrices of the DSSSDs, for each FARCOS telescope. The results have shown a good identification in charge up to $Z \approx 16$. Considering that FARCOS was placed between 13° and 30° in the laboratory frame system, an unambiguous isotopic identification of IMFs with atomic numbers up to $Z \approx 9$ and mass numbers up to $A \approx 20$ was achieved (see fig. 3).

3˙4. *Preliminary investigation of the isospin role in HI collisions.* – The investigation of isospin role in HI collisions is very preliminary at this point of the data analysis, because the results discussed above are related only to the data collected by FARCOS correlator. Nevertheless, a preliminary comparison of some mass distributions obtained from the particle identification phase revealed an interesting trend. In particular, for the "neutron-rich" $^{124}\mathrm{Sn} + {}^{64}\mathrm{Ni}$, the "neutron-poor" $^{112}\mathrm{Sn} + {}^{58}\mathrm{Ni}$ and the "isobaric" $^{124}\mathrm{Xe} + {}^{64}\mathrm{Zn}$, the comparison of mass distributions relating to the isotopes of Li, Be, B and C shows an effect of neutron enrichment for the neutron-rich system. The IMFs isospin distribution seems to follow the initial isospin content of the collided nuclei. However, this analysis must be considered preliminary, because it did not include the data collected by CHIMERA. At this phase of the data analysis, it was not possible to apply the selection of the global variables, that are mandatory for the characterization of the reaction mechanism (*i.e.*, the total charged particles multiplicity, the reaction plane, etc.). In the next step of the analysis, data will be filtered with the experimental setup features.

3˙5. *Preliminary results regarding the dynamical effects of the experiment.* – At this stage of the analysis, only events having particle multiplicity equal to one were considered and the detector response is not yet included. According to these experimental conditions, some distributions relating to the physics cases focused in the CHIFAR experiment were studied. Figure 4 illustrates the distribution of the perpendicular velocity as a function of the parallel velocity, for the "neutron-rich" system $^{124}\mathrm{Sn} + {}^{64}\mathrm{Ni}$. The IMFs with atomic charge $2 < Z < 16$ were selected. The emission of the IMFs is centered in the PLF velocity region (in the laboratory frame system), towards the mid-velocity. The forward and backward emission with respect to the PLF velocity highlights effects of the dynamical emission. Similar results were obtained for the other nuclear systems analysed in this experiment.

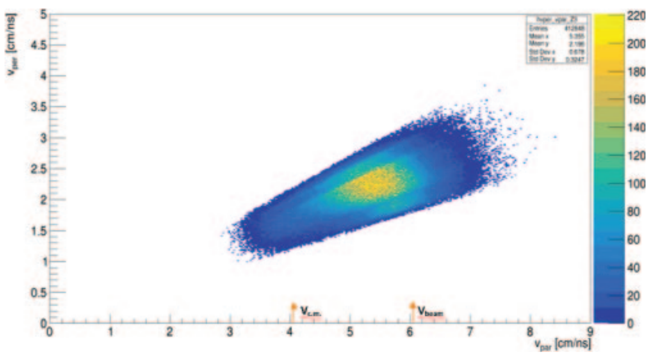

Fig. 4. – Distribution of the perpendicular velocity as a function of the parallel velocity, for the "neutron-rich" system ^{124}Sn + ^{64}Ni for IMFs with $2 < Z < 16$.

Mass number distribution as a function of the parallel velocity allows to confirm the dynamical effects and the good identification of the phase space for $2 < Z < 16$. The LCPs will be identified with specific methods applied to the data collected by the CsI(Tl) crystals in a next step of the analysis, and they are not included in the spectrum in fig. 5. The region between the center-of-mass velocity and the beam velocity was reconstructed quite well thanks to the high resolution of the FARCOS correlator.

Three isotope ratios were chosen, corresponding to the isotopes of Be, B and C. The N/Z distributions as a function of the parallel velocity for the three main systems, which means the "neutron-rich" ^{124}Sn + ^{64}Ni, the "neutron-poor" ^{112}Sn + ^{58}Ni and the "isobaric" ^{124}Xe + ^{64}Zn, were compared in fig. 6 for the carbon isotope ratio. The plot shows that the N/Z distributions follow the isospin content of the colliding nuclei, the memory of the initial conditions was not lost. The effect of the neutron enrichment is highlighted in each reaction, according to the respective isospin ratio (see table I). The analysis did not include the experimental setup efficiency, but in this preliminary phase the trend can be considered in agreement with the typical effects of dynamical emission.

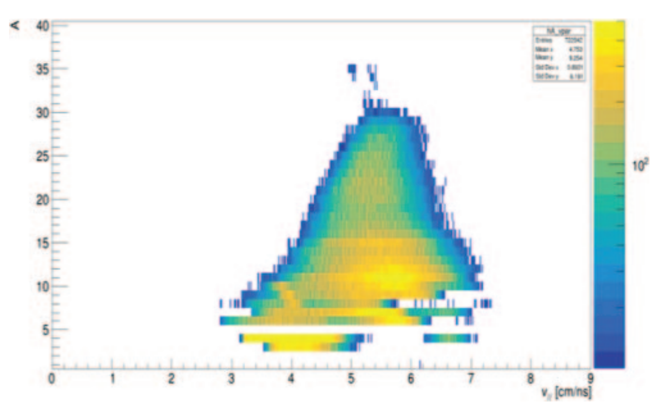

Fig. 5. – Mass number distribution as a function of the parallel velocity, for the ^{124}Sn + ^{64}Ni system.

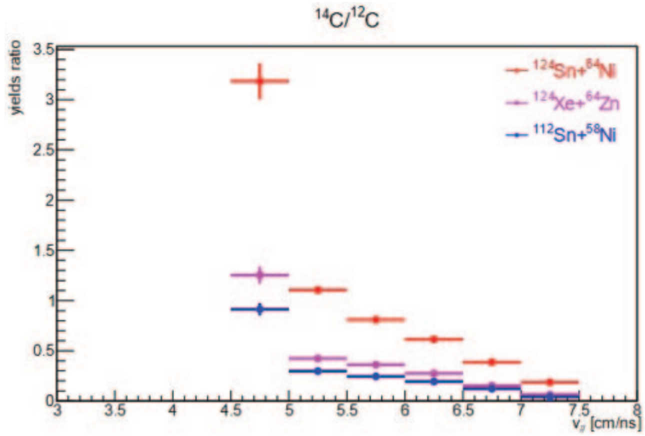

Fig. 6. – The carbon isotopes yield ratio as a function of the parallel velocity for $^{124}\mathrm{Sn} + {}^{64}\mathrm{Ni}$, $^{112}\mathrm{Sn} + {}^{58}\mathrm{Ni}$ and $^{124}\mathrm{Xe} + {}^{64}\mathrm{Zn}$ systems.

REFERENCES

[1] Pagano A. *et al.*, *Nucl. Phys. A*, **734** (2004) 504.
[2] De Filippo E. and Pagano A., *Eur. Phys. J. A*, **50** (2014) 32 and references therein.
[3] Russotto P. *et al.*, *Eur. Phys. J. A*, **56** (2020) 12.
[4] Pagano E. V. *et al.*, Proposal of CHIFAR experiment approved by the 2017 LNS-PAC.
[5] Pagano E. V. *et al.*, *EPJ Web of Conferences*, **117** (2016) 10008.
[6] Acosta L. *et al.*, *2019 IEEE Nuclear Science Symposium (NSS) and Medical Imaging Conference (MIC)* (IEEE) 2019, pp. 1–4.
[7] FARCOS Collaboration (Castoldi A., Guazzoni C. and Parsani T.), *Nuovo Cimento C*, **41** (2018) 168.
[8] Pollacco E. C. *et al.*, *Nucl. Instrum. Methods A*, **887** (2018) 81.
[9] De Filippo E. *et al.*, *Phys. Rev. C*, **71** (2005) 064604.
[10] Badalà A. *et al.*, *Riv. Nuovo Cimento*, **45** (2022) 189.
[11] Pagano A. *et al.*, *Eur. Phys. J. A*, **56** (2020) 102.
[12] Pagano E. V. *et al.*, *J. Phys.: Conf. Ser.*, **1014** (2018) 012011.
[13] Martorana N. S. *et al.*, *Phys. Lett. B*, **782** (2018) 112.
[14] Cardella G. *et al.*, *Phys. Rev. C*, **104** (2021) 064315.
[15] Cardella G. *et al.*, *Nucl. Phys. A*, **1020** (2022) 122395.
[16] `http://lise.nscl.msu.edu/lise.html`.